Eur. Phys. J. Plus (2018) **133**: 288
DOI 10.1140/epjp/i2018-12150-7

THE EUROPEAN PHYSICAL JOURNAL PLUS

Regular Article

Investigation of the thermal and microstructural changes of CuAlNiNb quaternary shape memory alloys by different niobium amount

Z. Deniz Cırak[1,a] and Mediha Kök[2]

[1] Inonu University, Vocational School of Health Service, Malatya, Turkey
[2] Fırat University, Faculty of Science, Department of Physics, Elazığ, Turkey

Received: 11 April 2018 / Revised: 3 June 2018
Published online: 30 July 2018

Abstract. Among the CuAl-based alloys, the most useful one is the CuAlNi ternary shape memory alloy. There are studies on the development of these alloys. In this study, β-Nb element was added to the CuAlNi alloy as a fourth element at various rates. The effect of the doped Nb element on the martensitic transformation temperature of the CuAlNi-shape memory alloy was determined by differential scanning calorimetry (DSC). When the value of transformation temperature in quaternary CuAlNi alloys increased, as a result, austenite start and martensite start temperatures are close to each other. Crystalline structure analysis with X-ray diffractometer revealed that $\beta 1'$ and $\gamma 1'$ phases were found in $Cu_{83.5}Ni_{3.5}Al_{13}$ alloy, which is the main alloy, while crystal structure of β-Nb phase was also found with Nb addition. Likewise, the same phases were determined by SEM-EDX analysis. In addition, the result of Vickers hardness measurements indicated that the hardness value of CuAlNi alloys increased by extent of contribution of Nb.

Introduction

Shape memory alloy is a family member of smart materials that shows two important properties, as shape memory effect and super-elasticity. These properties stem from the reversible martensite transformation and occur between high-temperature phase (austenite) and low-temperature phase (martensite). Because of these characteristic properties, they are among the material groups that are preferred in biomedical, automotive and airplane industries [1,2].

There is an extremely great demand for Cu-based shape memory alloys in practical applications due to their unique super-elasticity property and damping capability. Copper-based shape memory alloys have been investigated since 1970 and studies are still being conducted to improve them. Generally, Cu-Zn– and Cu-Al–based shape memory alloys are the most used. Among these, no doubt, there is an extremely great demand for Cu-Al-Ni shape memory alloy in high-temperature applications [3–6].

In the CuAlNi alloy, the chemical composition highly affects shape memory effect and transformation temperature value. In particular, the changes in aluminum or nickel elements cause serious effects. For instance, while the rate of Al exceeding 12% by mass can improve mechanical properties of the CuAlNi alloy, however, increasing the Ni rate by mass causes the alloy to become more fragile [7]. There are many factors affecting the temperature characteristic properties of CuAlNi alloys. Some of these are addition of another element, ageing effect and production techniques [4]. In addition, the CuAlNi alloy is generally used in applications that require working temperatures around 470 K and it has a wide and high hysteresis compared to the NiTi alloy. However, the fragility of the CuAlNi alloy increases for nickel composition above 4% by mass [8–10].

Saud *et al.* [8] added Ti, Co and Mn, separately at several rates, into the CuAlNi alloy and concluded that the alloy with cobalt addition showed the best transformation temperature, ductility and shape memory properties. In the same year, Saud and his colleagues [11] examined the properties of the CuAlNi alloy by adding Co at various ratios and, thus, they could determine that the 1% cobalt-doped CuAlNi alloy is the most optimal composition rate. Likewise, his team [12] studied the effect of Ti addition on the properties of the CuAlNi alloy.

[a] e-mail: deniz.yakinci@inonu.edu.tr (corresponding author)

In 2017, Saud *et al.* [9] produced CuAlNi-xTa ($x = 1, 2$ and 3 wt.%) alloys by powder metallurgy, microwave sintering and mechanical alloying methods and, then, examined the thermal and mechanical properties of those alloys by comparing all variations made in their crystal structures. Besides, Zhang *et al.* [13], by using the arc melting process, made a group of (Cu-13.0Al-4.0Ni)-xGd alloys with $x = 0, 0.3, 0.9, 1.5$ and 6 (wt.%). The reason for the choice of the Gd element is to improve the microstructure and mechanical properties of the CuAlNi shape memory alloy. They observed that Gd addition into the CuAlNi alloy showed a slight decrease in the transformation temperature and the mechanical properties of the CuAlNi alloy enhanced due to a slight decrease in the grain structure. In addition, Zare and coworkers [14] studied the effect of the chromium element on transformation, mechanical and corrosion behavior of thermomechanically induced Cu-Al-Ni shape memory alloys. In the present study, the effects of adding the β phase niobium (Nb) element on the thermal, microstructure and mechanical properties of the CuAlNi shape memory alloy were investigated.

Experiment

A group of $Cu_{83.5-x}Ni_{3.5}Al_{13}Nb_x$ ($x = 0, 1, 2, 3, 4$, % by mass) shape memory alloys were produced firstly by mixing with the powder of high-pure (99.8%) copper, nickel, aluminum and niobium at certain rates to obtain pellets; secondly, they were melted in an arc melting furnace. The melting process was repeated several times with the arc melting furnace to ensure that the alloys were homogenized. Thirdly, the produced $Cu_{83.5-x}Ni_{3.5}Al_{13}Nb_x$ ($x = 0, 1, 2, 3, 4$, % by mass) alloys were kept in a muffle furnace for 24 hours at 900 °C to ensure homogenization. Fourthly, after the alloys were taken out from the furnace, they were immediately submerged in salty-iced water as a sudden cooling process. Fifthly, to examine the thermoelastic martensite properties of the alloys, a Perkin-Elmer sapphire differential scanning calorimetry (DSC) device was used. The DSC measurements were performed at a rate of 10 °C/min for the heating-cooling process and run with 100 ml pure argon gas. Sixthly, at room temperature, the crystal structure of the alloys was specified by a Rigaku brand X-Ray analysis device with scanning rate of 4 °/min and for a range of 0 to 80 degrees. Seventhly, changes in the microstructure of Nb-doped CuAlNi alloys were determined by scanning electron microscopy (SEM). In addition, SEM-EDX measurements have also been used to verify that the elements were homogeneously dispersed in the alloy and to determine the presence of new precipitate phases. Finally, the hardness values of the alloys were measured with the Vickers microhardness measurement device by applying 200 gf.

Results and discussion

Thermal analysis measurements with DSC were performed at a temperature range between 50 and 350 °C to determine the martensite phase transformation temperatures of $Cu_{83.5-x}Ni_{3.5}Al_{13}Nb_x$ ($x = 0, 1, 2, 3, 4$, per mass) shape memory alloys. The heat flow curves obtained from the DSC measurements are shown in fig. 1 and the results of thermal measurements are given in table 1. According to table 1, the alloy with the lowest austenite $\leftrightarrow$ martensite transformation temperatures is the $Cu_{83.5}Ni_{3.5}Al_{13}$ main alloy, which has the highest enthalpy change (ΔH) observed. With the addition of the Nb element instead of the Cu element, the transformation temperatures increased and the difference between $A_f - M_f$ increased, but the value of ΔH decreased for quaternary CuAlNiNb alloys. The variation of the austenite/martensite transformation temperatures, according to the ratio of the Nb element, is given in fig. 2. This figure shows that, as the Nb ratio increases, the value of transformation temperature increases. The results are similar to the study conducted by Saud *et al.* [9], when they added the tantalum element to the CuAlNi alloy, and they observed that the value of austenite and martensite transformation temperatures increases with increasing the rate of Ta. On the other hand, the studies were conducted on NiTiCu and TiMoGa alloys, illustrating that adding Nb could reduce the transformation temperature values for both alloys [15,16]. The current study shows that the alloys with highest austenite start and martensite start temperatures are $Cu_{82.5}Ni_{3.5}Al_{13}Nb_1$ and $Cu_{80.5}Ni_{3.5}Al_{13}Nb_3$, which are different from the others, whereby their martensite start temperature are higher than the austenite start temperature. The austenite start temperature and martensite start temperature are very close to each other in $Cu_{81.5}Ni_{3.5}Al_{13}Nb_2$ shape memory alloys, they are even the same. Similar results were also reported in the study conducted by Fu *et al.* [17], who observed that the addition of Nb to the NiTi alloy leads to narrowing temperature hysteresis.

X-ray diffractograms of $Cu_{83.5-x}Ni_{3.5}Al_{13}Nb_x$ ($x = 0, 1, 2, 3, 4$) alloys taken at room temperature are given in fig. 3. The X-ray measurements were analyzed, for the CuAlNi alloy by use of the JCPDS card no: 050-1477, 28-0005, and, for Nb, by use of the JCPDS card no: 35-0789 and the literature [18,19]. Only the $\gamma 1'$ and $\beta 1'$ martensite phases were detected in the main CuAlNi shape memory alloy. These phases are known as the thick- and thin-plate martensite phases. With the addition of the Nb element, again, two martensite plates were observed. Together with these martensite plates, β-Nb phases were also found [8,11,12,16].

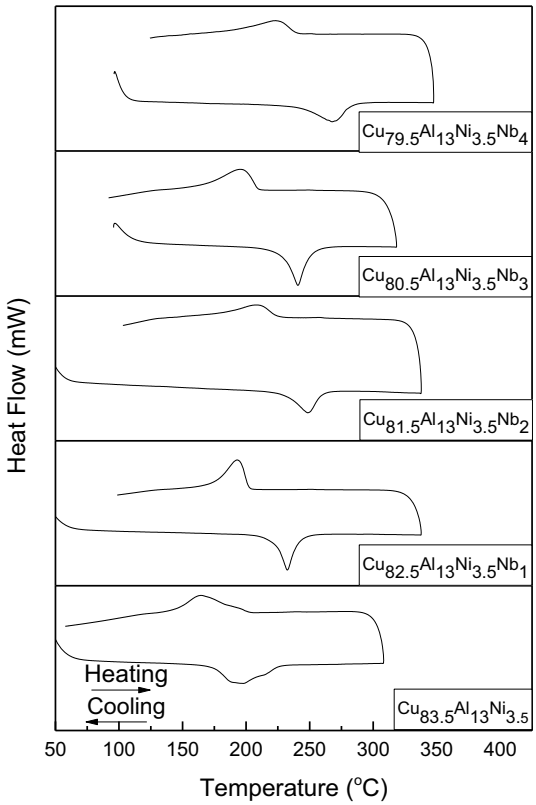

Fig. 1. Heat flux curves of $Cu_{83.5-x}Ni_{3.5}Al_{13}Nb_x$ $(x = 0, 1, 2, 3, 4)$ alloys during heating and cooling.

Table 1. Transformation temperatures and enthalpy change of $Cu_{83.5-x}Ni_{3.5}Al_{13}Nb_x$ $(x = 0, 1, 2, 3, 4)$ alloys.

	A_s (°C)	A_f (°C)	M_s (°C)	M_f (°C)	$A_f - M_f$ (°C)	ΔH_{ave} (J/g°C)
$Cu_{83.5}Al_{13}Ni_{3.5}$	174.0	226.1	193.8	146.4	79.7	10.4
$Cu_{82.5}Al_{13}Ni_{3.5}Nb_1$	219.7	244.0	202.2	176.6	67.4	9.4
$Cu_{81.5}Al_{13}Ni_{3.5}Nb_2$	224.2	262.6	225.5	186.2	76.4	5.0
$Cu_{80.5}Al_{13}Ni_{3.5}Nb_3$	224.6	256.3	208.5	166.3	90.0	8.8
$Cu_{79.5}Al_{13}Ni_{3.5}Nb_4$	235.1	284.0	239.3	190.8	93.2	5.3

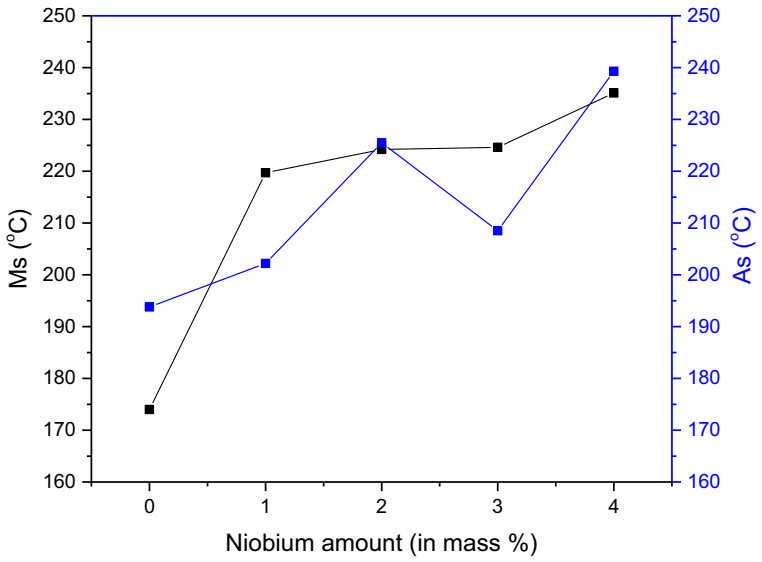

Fig. 2. The changes of transformation temperature of CuAlNi alloys with different amount of Nb.

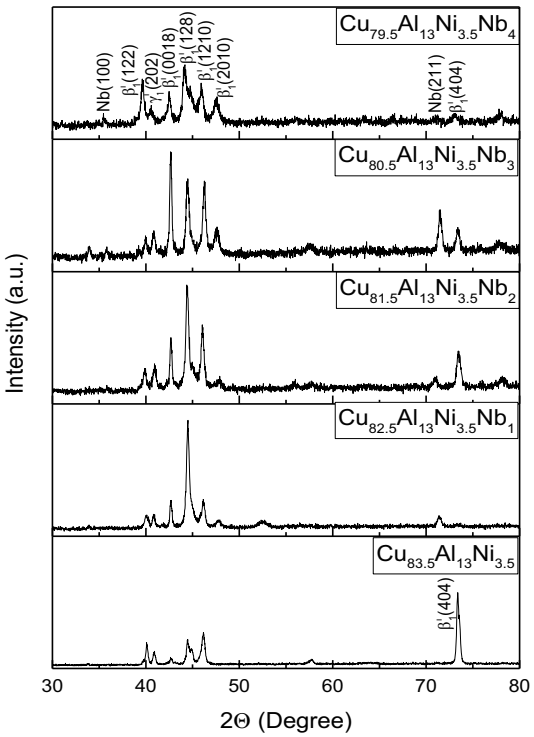

Fig. 3. X-ray diffractograms of $Cu_{83.5-x}Ni_{3.5}Al_{13}Nb_x$ $(x = 0, 1, 2, 3, 4)$ shape memory alloys taken at room temperature.

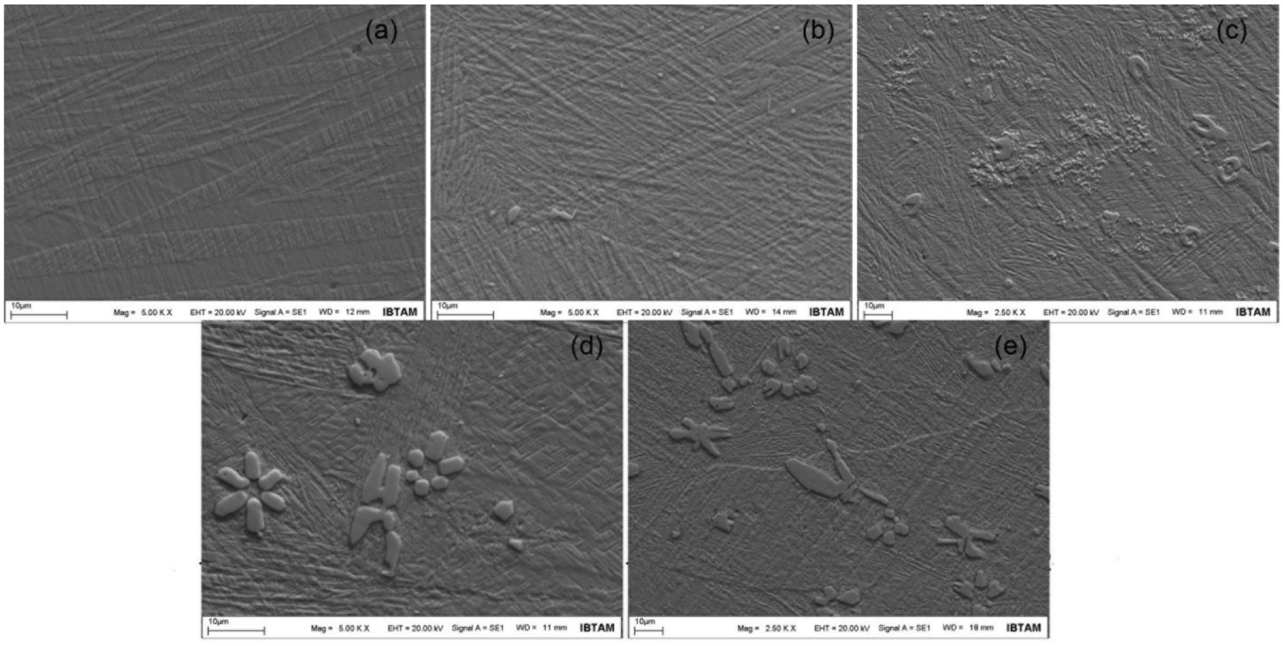

Fig. 4. SEM images of (a) $Cu_{83.5}Ni_{3.5}Al_{13}$; (b) $Cu_{82.5}Ni_{3.5}Al_{13}Nb_1$; (c) $Cu_{81.5}Ni_{3.5}Al_{13}Nb_2$; (d) $Cu_{80.5}Ni_{3.5}Al_{13}Nb_3$, (e) $Cu_{79.5}Ni_{3.5}Al_{13}Nb_4$ alloys.

When the SEM images are analyzed, it is clearly seen that there are thin martensite ($\beta 1'$) and thick martensite ($\gamma 1'$) plates for the $Cu_{83.5}Ni_{3.5}Al_{13}$ shape memory alloy. These martensite plates were also observed in X-ray measurements, and comply with the literature [8,20]. Very few precipitation phases are seen in the CuAlNi alloy (fig. 4(b)) so that only 1%wt of niobium was added to it. When the EDX measurement was taken from this precipitation area, niobium was detected at a rate of 49.4%. However, mostly thin-thick martensite plates were detected. C-shaped areas and blistered areas were detected in the martensite plates in the CuAlNi alloy that included Nb at a rate of 2% by mass.

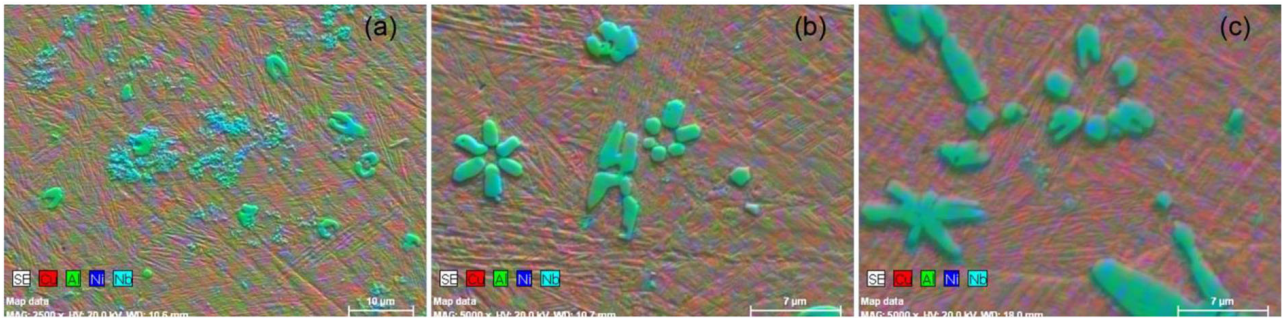

Fig. 5. Elemental mapping images of (a) $Cu_{81.5}Ni_{3.5}Al_{13}Nb_2$, (b) $Cu_{80.5}Ni_{3.5}Al_{13}Nb_3$, (c) $Cu_{79.5}Ni_{3.5}Al_{13}Nb_4$ shape memory alloys (red → copper; green → aluminum; blue → nickel; turquoise → niobium).

The Nb ratio in the blistered region was 57.9% by mass, and in the C-shaped region, the Nb ratio was 51.4% by mass. Furthermore, the phases with high Nb element ratio are β-Nb phases. It is clearly seen, in the SEM images (figs. 4(d)–(e)), that, when the mass percentage ratio of niobium increases from 3% to 4%, the blistered regions and C-shaped regions are transformed into flower- and clover-like shapes. These areas are placed on the martensite matrix. When chemical analysis is performed on the martensite area, niobium was not detected; in other words, this area only includes the CuAlNi phase. The chemical analyses with EDX determined that the Nb rate was around 49% in clover-like and C-shaped areas. When all results are considered as a whole, it is possible to claim that the Nb element formed precipitation phases in the CuAlNi shape memory alloy.

Finally, mapping analysis was performed on the SEM-EDX measurements of the CuAlNi alloys, whose niobium ratio was 2%, 3% and 4% (fig. 5). According to mapping results, it is clearly seen that there is excessive niobium in all of the precipitation phases. This result shows that the increasing Nb rate does not dissolve in the CuAlNi alloy, and thus it forms a precipitation phase.

The microhardness measurements of the alloys were made when all the alloys were in the martensite phase (at room temperature). The hardness values complied with those of the literature for $Cu_{83.5}Ni_{3.5}Al_{13}$ as fully martensite 240 HV [21]; for $Cu_{82.5}Ni_{3.5}Al_{13}Nb_1$, the value was 221 HV in the fully martensite area (the precipitations were in the size whose hardness value could not be measured). For $Cu_{81.5}Ni_{3.5}Al_{13}Nb_2$ alloy, the hardness value in the C-shaped precipitations was 381 HV, and 275 HV in the martensite area. In addition, $Cu_{80.5}Ni_{3.5}Al_{13}Nb_3$ had hardness values of 341 HV in its flower-shaped area, 423 HV in the clover-like area, and 271 HV in the martensite area. Also, quantitative values of hardness in $Cu_{79.5}Ni_{3.5}Al_{13}Nb_4$ was 351 HV in the flower-shaped area, 423 HV in the clover-like area, and 267 HV in the martensite area. There is a connection between the mapping and EDX measurement results and hardness measurement results as follows: the rate of niobium was nearly twice that of the other elements (Cu, Al, Ni) in the C-shaped, clover-like–shaped and flower-shaped areas. From the results, it can be concluded that niobium seriously increases the hardness value of the CuAlNi alloy and it also enhances the strength of the CuAlNi shape memory alloy [21].

Conclusions

The changes that occured as a result of adding β phase niobium into the CuAlNi shape memory alloy could be summarized as follows:

– It was observed that Nb additive residue, to the CuAlNi shape memory alloy, shows a higher transformation temperature and, also, the martensite start temperature approaches to the austenite start temperature. The CuAlNiNb shape memory alloy may be used in systems which are expected to give thermoelastic transformation within a short temperature range.

– When the crystal structure of the CuAlNiNb alloy is analyzed, it can be seen that new peaks belonging to a new phase emerge with the $\gamma 1'$ and $\beta 1'$ and martensite phases. This new phase was the β Nb phase which together with the other is supported by the SEM-EDX measurement results.

– Finally, the Vickers microhardness measurements of the alloys are made for the precipitation phases and for martensite phases seen in SEM images; the hardness values in martensite phase are nearly the same for all alloys, and it can also be observed that hardness values of the precipitation phase increase at a serious level with increasing the Nb element rate. This result shows that the CuAlNi alloy is strengthened with the addition of Nb.

References

1. J.P. Oliveira *et al.*, Mater. Design. **128**, 166 (2017).
2. P. La Roca *et al.*, Scr. Mater. **135**, 5 (2017).
3. S.N. Saud *et al.*, Metal. Mater. Trans. A **47**, 5242 (2016).
4. S.N. Saud *et al.*, J. Therm. Anal. Calorim. **123**, 377 (2016).
5. I. Ivanić *et al.*, Eng. Fail. Anal. **77**, 85 (2017).
6. N. Babacan *et al.*, Mater. Sci. Eng. A **701**, 352 (2017).
7. Y.C. Wee *et al.*, J. Teknol. **74**, 53 (2015).
8. S.N. Saud *et al.*, J. Mater. Res. **30**, 2258 (2015).
9. S.N. Saud *et al.*, Scanning **2017**, 1789454 (2017).
10. J.L. Liu *et al.*, Mater. Sci. Eng. A **696**, 315 (2017).
11. S.N. Saud *et al.*, Metal. Mater. Trans. A **46**, 3528 (2015).
12. S.N Saud *et al.*, J. Therm. Anal. Calorim. **118**, 111 (2014).
13. X. Zhang *et al.*, Mater. Lett. **180**, 223 (2016).
14. M. Zare *et al.*, J. Therm. Anal. Calorim. **127**, 2113 (2017).
15. H.Y. Kim *et al.*, Mater. Trans. **47**, 518 (2006).
16. G.C. Wang *et al.*, Intermetallics **72**, 30 (2016).
17. X. Fu *et al.*, Chin. J. Aeronaut. **22**, 658 (2009).
18. A.T. Adorno *et al.*, J. Therm. Anal. Calorim. **97**, 127 (2009).
19. A.G. Magdalena *et al.*, J. Therm. Anal. Calorim. **106**, 339 (2011).
20. N.S. Pascal *et al.*, Adv. Powder Technol. **28**, 2605 (2017).
21. S.M. Dar *et al.*, Tech. J., Univ. Eng. Technol. Taxila **22-2**, 9 (2017).